Probing gluon saturation with diffractive jets

Edmond Iancu

P. Caucal, S. Hauksson, A. Mueller, D. Triantafyllopoulos, S.-Y. Wei, F. Yuan
P. Gimeno-Estivill, M. Guerrero, T. Lappi, F. Salazar

2112.06353, 2207.06268, 2304.12401, 2402.14748, 2406.04238,
2408.03129, 2503.16162, 2510.08454, 2512.11730, 2606.04169

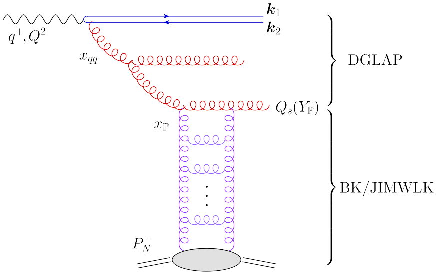

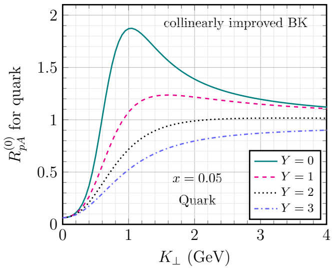

Dipole Picture for DIS at small x

- Cross-section = photon wavefunction $(\gamma^* \to q\bar{q}) \otimes$ dipole cross-section

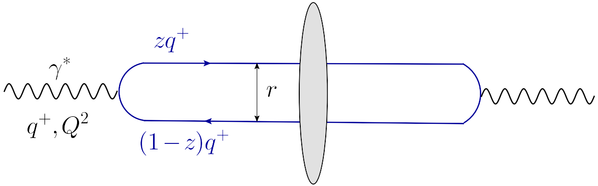

$$\sigma_{\gamma^* A}(Q^2, x) = \int \mathrm{d}^2 r \int_0^1 \mathrm{d}z \left|\Psi_{\gamma^* \to q\bar{q}}(r, z; Q^2)\right|^2 \underbrace{\sigma_{\text{dipole}}(r, A, x)}_{2\pi R_A^2\, T_A(r,x)}$$

- QCD dynamics encoded in the dipole amplitude $T_A(r, x)$

- Transition from weak to strong scattering at $r \sim 1/Q_s$:

$$T_A(r,x) \simeq \begin{cases} r^2 Q_s^2(A,x) & \text{for } rQ_s \ll 1 \text{ (color transparency)} \\ 1 & \text{for } rQ_s \gtrsim 1 \text{ (black disk/saturation)} \end{cases}$$

High energy evolution: BK/JIMWLK

- Decrease x starting at $x_0 \sim 10^{-2}$: non-linear generalisation of BFKL

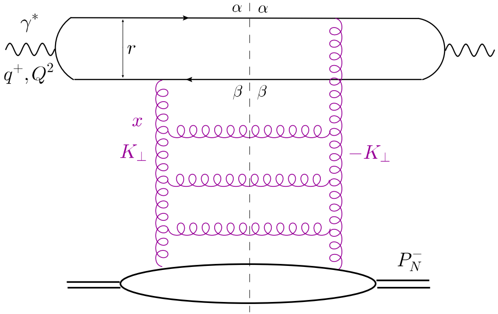

$$T_A(r,x) \simeq \begin{cases} \left(r^2 Q_s^2(A,x)\right)^{\gamma_s} & \text{for } rQ_s \ll 1 \text{ (weak scattering)} \\ 1 & \text{for } rQ_s \gtrsim 1 \text{ (black disk/saturation)} \end{cases}$$

$$Q_s^2(A,x) \simeq Q_s^2(p,x_0) A^{1/3} \left(\frac{x_0}{x}\right)^{\lambda_s}, \quad \lambda_s \simeq 0.25, \quad \gamma_s \simeq 0.63$$

Inclusive cross-section

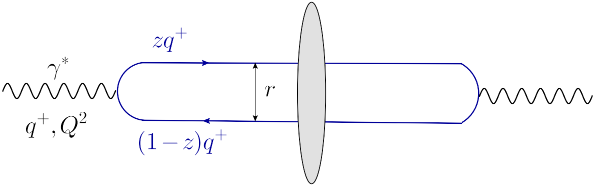

$$\sigma_{\gamma^* A}(Q^2, x) = \int \mathrm{d}^2 r \int_0^1 \mathrm{d}z \left|\Psi_{\gamma^* \to q\bar{q}}(r, z; Q^2)\right|^2 2\pi R_A^2 \, T_A(r, x)$$

- Competition between scattering and photon virtuality
  - strong scattering requires large dipoles: $r \gtrsim 1/Q_s$
  - virtuality limits the dipole size: $r \lesssim 1/\bar{Q}$ with $\bar{Q}^2 \equiv z(1-z)Q^2$
- Strong scattering/saturation dominates only for relatively low virtuality:

$$Q^2 \lesssim Q_s^2(A, x) \sim 1 \text{ GeV}^2 \quad \text{for } A \sim 200 \ \& \ x \sim 10^{-2}$$

- Possible contamination from non-perturbative physics: $\Lambda_{\rm QCD} \sim 0.2$ GeV

Elastic scattering

- Compare elastic scattering (left) and inelastic (right)

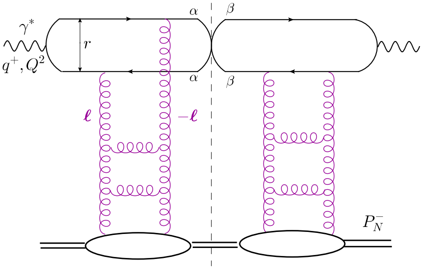

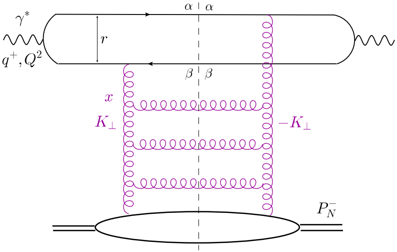

$$\sigma_{\rm el}(Q^2,x) = \int {\rm d}^2 r \int {\rm d}z \big|\Psi(r,z;Q^2)\big|^2\, 2\pi R_A^2\, |T(r,x)|^2$$

- Amplitude squared $\Longrightarrow$ Diffraction abhors weak scattering
- $\sigma_{\rm el}(Q^2,x)$ is controlled by strong scattering even when $Q^2 \gg Q_s^2(A,x)$
  - aligned jets: $r \sim 1/Q_s$ and $z(1-z) \sim Q_s^2/Q^2 \ll 1$

One vs two Pomerons... at HERA

- W/o saturation: σ_{el} would rise with $\frac{1}{x}$ (or with A) like two Pomerons

$$T^2 \simeq \left[r^2 Q_s^2(A,x)\right]^2 \propto \frac{A^{2/3}}{x^{2\lambda_s}} \qquad \text{vs.} \qquad T \simeq r^2 Q_s^2(A,x) \propto \frac{A^{1/3}}{x^{\lambda_s}}$$

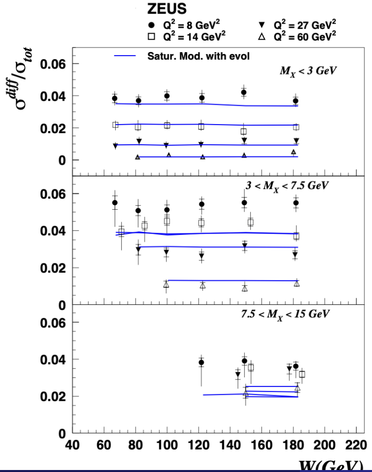

- But it doesn't! Double integral controlled by saturation: $T \sim 1$, or $r \sim 1/Q_s$
- Almost the same scaling as σ_{tot}:

$$\frac{\sigma_{el}}{\sigma_{tot}} \sim \frac{1}{\ln\left(Q^2/Q_s^2\right)}$$

- Weak x-dependence confirmed by HERA *(Bartels, Golec-Biernat, Kowalski, 2002)*
- Would be interesting to also check the A-dependence at the EIC

Diffractive particle production at high Q^2

- Leading order in α_s: a quark-antiquark pair in a colour singlet state
- Back-to-back in the transverse plane: $\boldsymbol{k}_{1\perp} = -\boldsymbol{k}_{2\perp} \equiv \boldsymbol{P}_\perp$
- Rapidity gap $Y_{\mathbb{P}} = \ln(1/x_{\mathbb{P}})$ between hadronic target and diffractive system

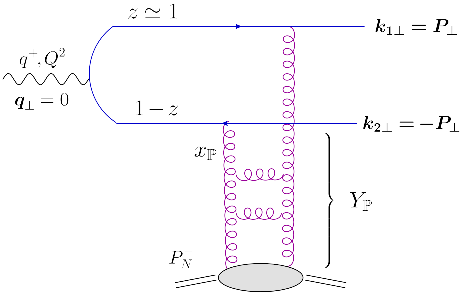

$$x_{\mathbb{P}} = \frac{Q^2 + M_{q\bar{q}}^2}{2P \cdot q} \ll 1$$

$$M_{q\bar{q}}^2 \simeq \frac{P_\perp^2}{z(1-z)} \sim Q^2$$

$$z(1-z) \sim \frac{Q_s^2(Y_{\mathbb{P}})}{Q^2} \ll 1$$

- Typical events: the produced particles are semi-hard: $P_\perp \sim 1/r \sim Q_s(Y_{\mathbb{P}})$
- "Aligned jet": the quark $(z \simeq 1)$ is aligned with the photon (forward)

Diffractive particle production at high Q^2

- Leading order in α_s: a quark-antiquark pair in a colour singlet state
- Back-to-back in the transverse plane: $\boldsymbol{k}_{1\perp} = -\boldsymbol{k}_{2\perp} \equiv \boldsymbol{P}_\perp$
- Rapidity gap $Y_{\mathbb{P}} = \ln(1/x_{\mathbb{P}})$ between hadronic target and diffractive system

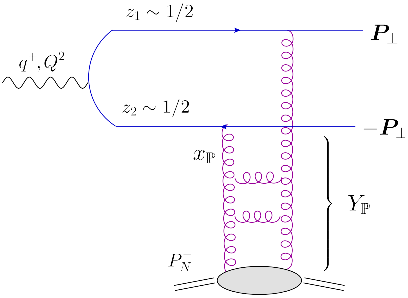

$$z_1 \sim z_2 \sim \frac{1}{2}\,, \qquad P_\perp \sim \frac{1}{r} \sim Q$$

$$\frac{\mathrm{d}\sigma_{\mathrm{el}}^{\gamma^* A \to q\bar{q}A}}{\mathrm{d}z_1 \mathrm{d}z_2 \mathrm{d}^2\boldsymbol{P}} \propto \underbrace{\alpha_{\mathrm{em}} r^2}_{\gamma^* \to q\bar{q}} \underbrace{Q_s^4 r^4}_{T_{q\bar{q}}^2}$$

$$P_\perp \sim \frac{1}{r} \Longrightarrow \frac{1}{P_\perp^6}$$

- Hard dijets ($P_\perp \sim Q$) are possible too, but higher twist: color transparency
- Most naturally produced via additional radiation: 2+1 jets

Diffractive SIDIS: TMD factorisation

- Mesure only the quark: leading-twist contribution at $Q^2 \gg P_\perp^2$
  - integral over z_2 controlled by "aligned jets": $z_2 \sim \frac{P_\perp^2}{Q^2} \ll 1$
- Soft antiquark can be viewed as a constituent of the target

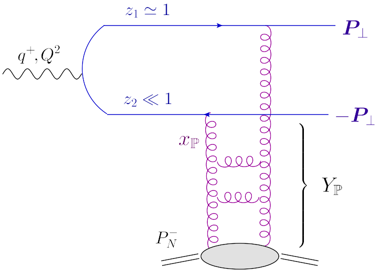

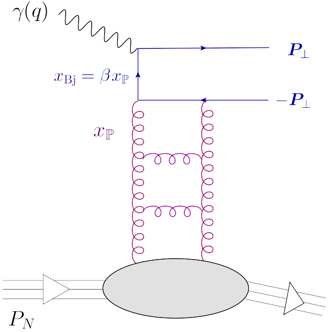

- Target picture: the Pomeron splits into a quark-antiquark pair $\pm \boldsymbol{P}$
  - t-channel quark absorbs the photon and becomes the aligned jet

Diffractive SIDIS: TMD factorisation

- Mesure only the quark: leading-twist contribution at $Q^2 \gg P_\perp^2$
  - integral over z_2 controlled by "aligned jets": $z_2 \sim \frac{P_\perp^2}{Q^2} \ll 1$
- Soft antiquark can be viewed as a constituent of the target

- change longitudinal variable: $z_2 \to \beta$
- longitudinal fraction w.r.t. Pomeron

$$\beta \equiv \frac{x_{\rm Bj}}{x_{\mathbb{P}}} = \frac{Q^2}{Q^2 + P_\perp^2/z_2}$$

$$\frac{d\sigma^{\gamma_T^* A \to qAX}}{d\ln(1/\beta)\, d^2\boldsymbol{P}} = \frac{8\pi^2 \alpha_{em} e_f^2}{Q^2}\, \mathcal{Q}_{\mathbb{P}}(\beta, Y_{\mathbb{P}}, P_\perp^2)$$

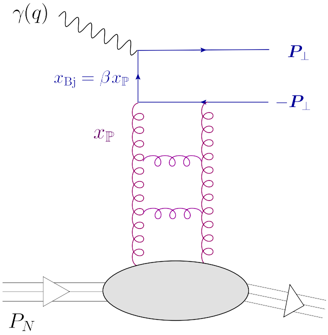

- Cross-section = Hard factor (γ^* absorption) $\times$ Quark DTMD

(Hatta, Xiao, Yuan, 2205.08060; Hauksson et al. 2402.14748)

The quark diffractive TMD

- Unintegrated quark distribution of the Pomeron (relabel $\beta \to x$) :

$$\mathcal{Q}_{\mathbb{P}}(x, Y_{\mathbb{P}}, P_\perp^2) \,=\, \frac{S_\perp N_c}{4\pi^3} \quad \underbrace{\Psi_{\mathbb{P}}(x, Y_{\mathbb{P}}, P_\perp^2)}_{\text{occupation number}}$$

- Bessel-Fourier transform of the dipole amplitude $T(r, Y_{\mathbb{P}})$

$$\Psi_{\mathbb{P}}(x, Y_{\mathbb{P}}, P_\perp^2) \simeq x \begin{cases} 1, & P_\perp \lesssim \tilde{Q}_s(x, Y_{\mathbb{P}}) \\[2ex] \dfrac{\tilde{Q}_s^4(x, Y_{\mathbb{P}})}{P_\perp^4}, & P_\perp \gg \tilde{Q}_s(x, Y_{\mathbb{P}}) \end{cases}$$

- Rapid decay $\sim 1/P_\perp^4$ at $P_\perp^2 \gg \tilde{Q}_s^2(x, Y_{\mathbb{P}}) \equiv (1-x) Q_s^2(Y_{\mathbb{P}})$

- Quark diffractive PDF (hence F_2^D) controlled by saturation: $P_\perp \sim \tilde{Q}_s$

$$x q_{\mathbb{P}}(x, x_{\mathbb{P}}, Q^2) \equiv \int^{Q^2} \mathrm{d}P_\perp^2 \, \mathcal{Q}_{\mathbb{P}}(x, Y_{\mathbb{P}}, P_\perp^2) \,\propto\, x(1-x)\, Q_s^2(Y_{\mathbb{P}}) \,\propto\, A^{1/3}$$

Numerical results *(2402.14748)*

- Left: McLerran-Venugopalan model. Right: BK evolution with $Y_{\mathbb{P}}$
- $\Psi_{\mathbb{P}}(x, Y_{\mathbb{P}}, K_\perp^2)$ multiplied by $K_\perp$: Pronounced maximum at $K_\perp \simeq \tilde{Q}_s$

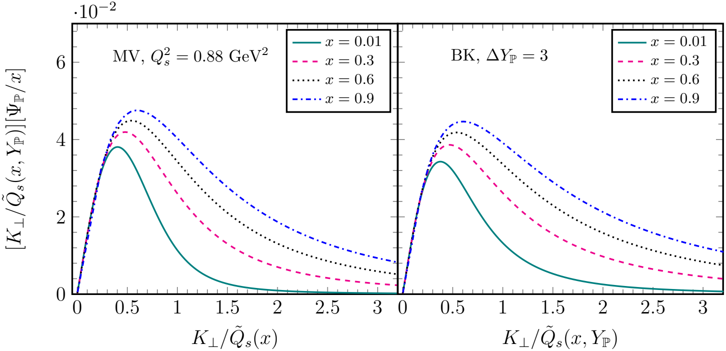

- BK evolution: increasing $Q_s(Y_{\mathbb{P}})$, approximate geometric scaling
  - (roughly) a function of the ratio $K_\perp/\tilde{Q}_s(x, Y_{\mathbb{P}})$
  - small anomalous dimension $1/K^{4\gamma_s}$ with $\gamma_s \sim 0.63$

The R_{pA} ratio for diffractive SIDIS *(2606.04169)*

- The ratio the D-SIDIS cross-sections in eA and respectively ep
  - TMD factorisation $\Rightarrow$ the ratio of the respective TMDs
  - normalised to unity at large $K_\perp \gg Q_s(A) = 1$ GeV

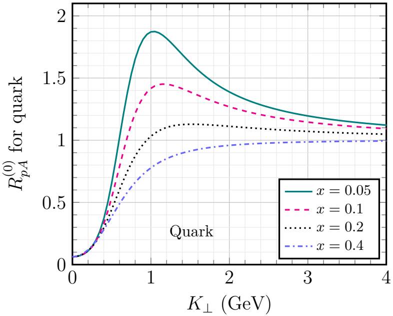

$$R_{pA}(x, Y_{\mathbb{P}}, K_\perp) \equiv \frac{\Psi_{\mathbb{P}}^{(A)}(x, x_{\mathbb{P}}, K_\perp^2)}{A^{2/3}\Psi_{\mathbb{P}}^{(p)}(x, x_{\mathbb{P}}, K_\perp^2)}$$

$$Q_s^4(A) = A^{2/3}\, Q_s^4(p)$$

Peak height $R_{\max} \sim \ln^2 \dfrac{Q_s^2(A)}{\Lambda^2}$

- Suppression at $K_\perp < Q_s$ and Cronin peak at $K_\perp \simeq Q_s$: saturation
- The peak disappears with increasing x: two competing mechanisms

The R_{pA} ratio for diffractive SIDIS (2606.04169)

- The ratio the D-SIDIS cross-sections in eA and respectively ep
  - TMD factorisation $\Rightarrow$ the ratio of the respective TMDs
  - normalised to unity at large $K_\perp \gg Q_s(A) = 1$ GeV

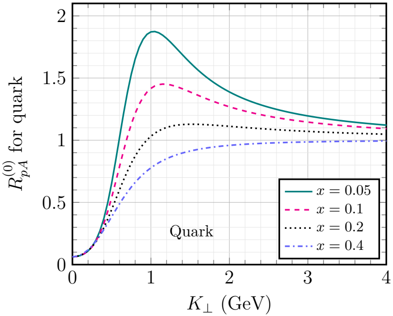

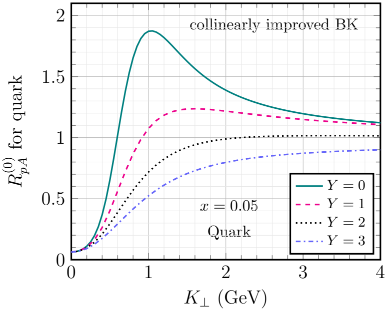

- Suppression at $K_\perp < Q_s$ and Cronin peak at $K_\perp \simeq Q_s$: saturation
- It also disappears with increasing $Y_{\mathbb{P}}$ for a given x: proton evolves faster

2+1 diffractive jets (2112.06353, 2207.06268)

- "Hard jets": cross-section with leading-twist power-tail at large $P_\perp \gg Q_s$
  - $1/P_\perp^2$ for single jets, $1/P_\perp^4$ for dijets ...
- Naturally produced via a hard splitting: e.g. $q \to q + g$ or $\gamma \to q\bar{q}$

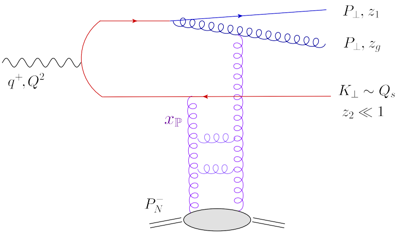

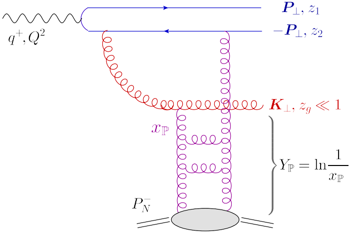

- A hard dijet ($P_\perp \gg Q_s$) accompanied by a semi-hard ($K_\perp \sim Q_s$) parton
  - the 3-parton system undergoes strong elastic scattering
- Large effective dipole ($q\bar{q}$, or gg), with $r \sim 1/Q_s$, hence $T(r) \sim 1$

TMD factorisation for 2+1 jets (2402.14748)

- The semi-hard parton can be transferred to the target: $x = \frac{x_{qg}}{x_{\mathbb{P}}}$ or $x = \frac{x_{q\bar{q}}}{x_{\mathbb{P}}}$

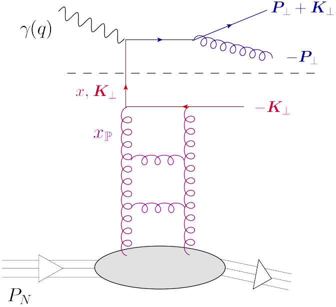

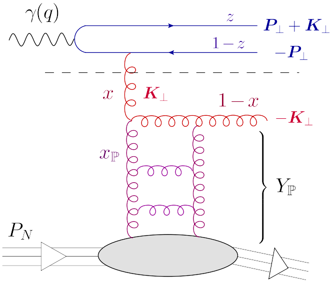

$$\frac{d\sigma^{\gamma_T^* A \to qg(\bar{q})A}}{dz\, d^2\boldsymbol{P}\, d^2\boldsymbol{K}\, d\ln(1/x)} = H_{qg}(P_\perp^2)\, \mathcal{Q}_{\mathbb{P}}(x, x_{\mathbb{P}}, K_\perp^2) + H_{q\bar{q}}(P_\perp^2)\, \mathcal{G}_{\mathbb{P}}(x, x_{\mathbb{P}}, K_\perp^2)$$

- Hard factors $H_{qg}(P_\perp^2)\,, H_{q\bar{q}}(P_\perp^2)$ which decrease like $1/P_\perp^4$

- The same as for inclusive dijets

TMD factorisation for 2+1 jets (2402.14748)

- The semi-hard parton can be transferred to the target: $x = \frac{x_{qg}}{x_{\mathbb{P}}}$ or $x = \frac{x_{q\bar{q}}}{x_{\mathbb{P}}}$

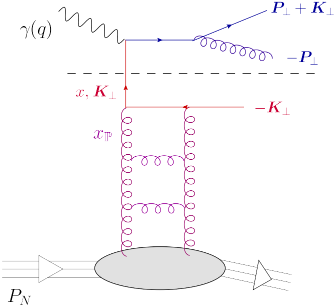

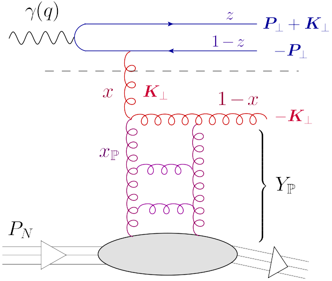

$$\frac{d\sigma^{\gamma_T^* A \to qg(\bar{q}) A}}{dz\, d^2\boldsymbol{P}\, d^2\boldsymbol{K}\, d\ln(1/x)} = H_{qg}(P_\perp^2)\, \mathcal{Q}_{\mathbb{P}}(x, x_{\mathbb{P}}, K_\perp^2) + H_{q\bar{q}}(P_\perp^2)\, \mathcal{G}_{\mathbb{P}}(x, x_{\mathbb{P}}, K_\perp^2)$$

- The same quark DTMD $\mathcal{Q}_{\mathbb{P}}(x, x_{\mathbb{P}}, K_\perp^2)$ as in SIDIS: universality

- Gluon DTMD $\mathcal{G}_{\mathbb{P}}(x, x_{\mathbb{P}}, K_\perp^2)$: UGD of the Pomeron

NLO corrections to diffractive SIDIS *(2402.14748)*

- Assume $Q^2 \gg P_\perp^2 \gg Q_s^2$ and measure only the hard quark
  - integrate out the other hard parton: NLO, but leading-twist tail $1/P_\perp^2$
- From $z_g \sim P_\perp^2/Q^2$ to $\xi \Rightarrow$ DGLAP splitting functions: $P_{qq}(\xi)$ & $P_{qg}(\xi)$

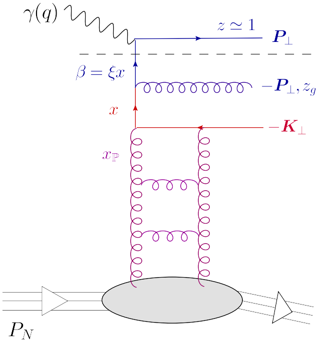

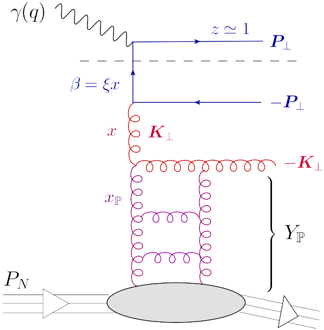

- Target evolution recovered from the evolution of the photon projectile

NLO corrections to diffractive SIDIS *(2402.14748)*

- Assume $Q^2 \gg P_\perp^2 \gg Q_s^2$ and measure only the hard quark
  - integrate out the other hard parton: NLO, but leading-twist tail $1/P_\perp^2$
- From $z_g \sim P_\perp^2/Q^2$ to $\xi \Rightarrow$ DGLAP splitting functions: $P_{qq}(\xi)$ & $P_{qg}(\xi)$

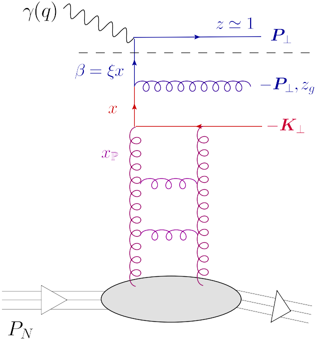

- BK/JIMWLK over the rapidity gap $Y_{\mathbb{P}}$
- CSS & DGLAP for the diffractive system
- DGLAP for quark DPDF: $\ln P_\perp^2$
- CSS for quark DTMD: $\ln Q^2$
- MV+BK $\Rightarrow$ initial conditions for CSS+DGLAP

$$\Delta\mathcal{Q}_{\mathbb{P}}(\beta, x_{\mathbb{P}}, P_\perp^2) = \frac{\alpha_s C_F}{2\pi^2}\,\frac{1}{P_\perp^2}\int_\beta^{1-\xi_0} \mathrm{d}\xi\, \frac{1+\xi^2}{1-\xi}\,\frac{\beta}{\xi} q_{\mathbb{P}}\left(\frac{\beta}{\xi}, x_{\mathbb{P}}, P_\perp^2\right)$$

Separating CSS from DGLAP *(2408.03129)*

- Measure a quark jet $\Rightarrow$ only large-angle emissions matter

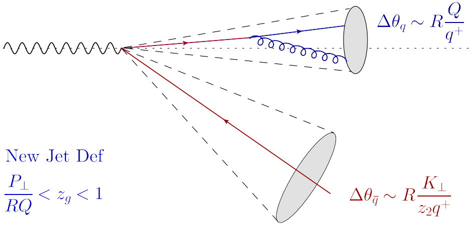

$$\Delta\theta_{qg} \simeq \frac{P_\perp}{z_g q^+} > \frac{Q}{q^+}$$

$$z_g \leq \frac{P_\perp}{Q} \ll 1$$

$$\Longrightarrow\ 1-\xi \geq \xi_0 \equiv \frac{P_\perp}{Q}$$

- Logarithmic dependence upon ξ_0: expand for small ξ_0

$$\Delta\mathcal{Q}_{\mathbb{P}}(\beta, x_{\mathbb{P}}, P_\perp^2, Q^2) = \frac{\alpha_s C_F}{2\pi^2}\ln\frac{Q^2}{P_\perp^2}\,\frac{\beta q_{\mathbb{P}}\left(\beta, x_{\mathbb{P}}, P_\perp^2\right)}{P_\perp^2}$$
$$+\frac{\alpha_s C_F}{2\pi^2}\frac{1}{P_\perp^2}\int_\beta^1 \mathrm{d}\xi\,\frac{1+\xi^2}{(1-\xi)_+}\,\frac{\beta}{\xi}q_{\mathbb{P}}\left(\frac{\beta}{\xi}, x_{\mathbb{P}}, P_\perp^2\right) + \mathcal{O}(\xi_0)$$

- Add the virtual corrections: the perturbative Sudakov *(cf. talk by Feng)*

CSS evolution for diffraction *(2512.11730)*

- Solve CSS in $b_\perp$-space: no need for non-perturbative Sudakov

$$\mathcal{F}_g(x, P_\perp, Q^2) = \int \mathrm{d}^2\boldsymbol{b}\; \mathrm{e}^{-i\boldsymbol{P}\cdot\boldsymbol{b}}\, \tilde{\mathcal{F}}_g^{(0)}(x, \boldsymbol{b}) \exp\left[-\frac{\alpha_s N_c}{4\pi} \ln^2 \frac{Q^2}{\mu_b^2}\right]$$

- $\tilde{\mathcal{F}}_g^{(0)}(x, b_\perp) \propto 1/(Q_s b_\perp)^8$: rapid decay at large $b_\perp$, due to saturation

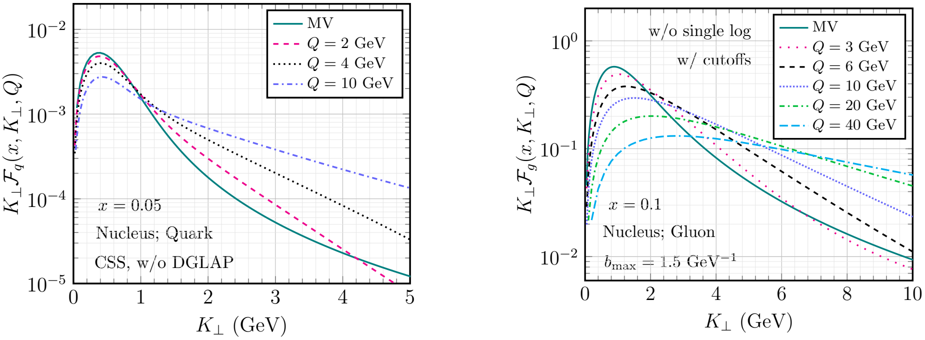

- CSS without DGLAP. Left: Quark DTMD. Right: Gluon DTMD

CSS evolution for R_{pA} *(w.i.p. w/ Dionysis and Shu-Yi)*

- The CSS/DGLAP evolution changes the tail of the DTMDs at large $P_\perp$:

$$\frac{Q_s^4(A,Y_{\mathbb{P}})}{P_\perp^4} \sim \frac{A^{2/3}}{P_\perp^4} \longrightarrow \frac{\alpha_s C_F}{2\pi^2} \ln\frac{Q^2}{P_\perp^2} \frac{\beta q_{\mathbb{P}}\left(\beta, x_{\mathbb{P}}, P_\perp^2, A\right)}{P_\perp^2} \sim \frac{A^{1/3}}{P_\perp^2}$$

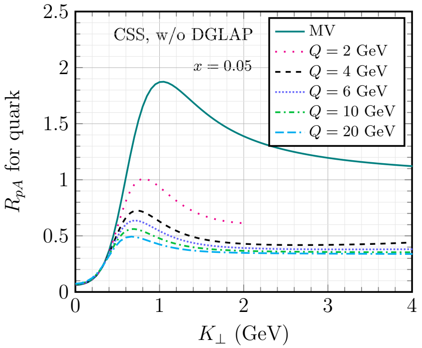

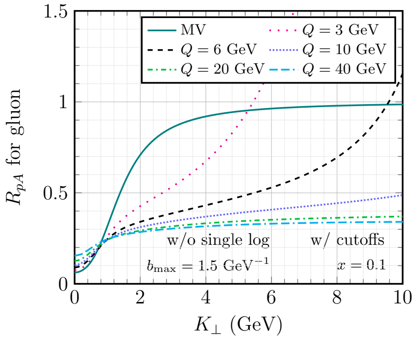

- The peak is strongly suppressed, yet still visible
- At large $K_\perp \gg Q_s(A)$, the ratio approaches $R_{pA} = 1/A^{1/3}$

CSS evolution for R_{pA} *(w.i.p. w/ Dionysis and Shu-Yi)*

- The CSS/DGLAP evolution changes the tail of the DTMDs at large $P_\perp$:

$$\frac{Q_s^4(A,Y_{\mathbb{P}})}{P_\perp^4} \sim \frac{A^{2/3}}{P_\perp^4} \longrightarrow \frac{\alpha_s C_F}{2\pi^2} \ln \frac{Q^2}{P_\perp^2} \frac{\beta q_{\mathbb{P}}\left(\beta, x_{\mathbb{P}}, P_\perp^2, A\right)}{P_\perp^2} \sim \frac{A^{1/3}}{P_\perp^2}$$

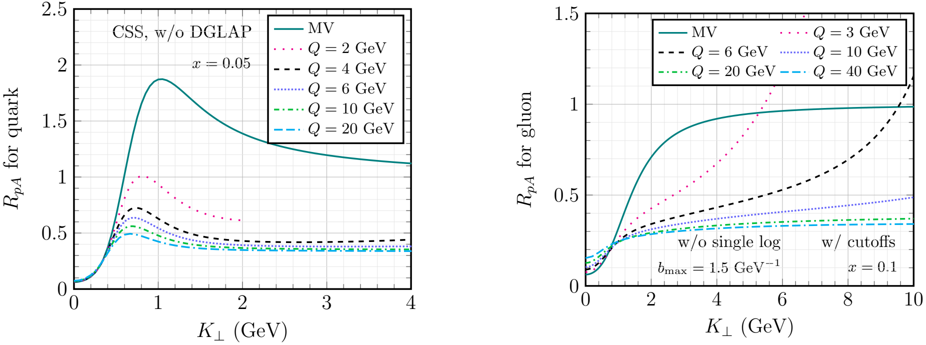

- For the gluon DTMD, there is no Cronin peak
- At large $K_\perp \gg Q_s(A)$, the ratio approaches $R_{pA} = 1/A^{1/3}$

- The DGLAP solution enters the boundary condition for CSS

$$\mathcal{Q}_{\mathbb{P}}(x, x_{\mathbb{P}}, K_\perp^2, Q^2) = \Bigg\{ \mathcal{Q}_{\mathbb{P}}^{(0)}(x, x_{\mathbb{P}}, K_\perp^2) + \frac{\alpha_s C_F}{2\pi^2} \ln\frac{Q^2}{K_\perp^2} \frac{x q_{\mathbb{P}}\left(x, x_{\mathbb{P}}, P_\perp^2\right)}{K_\perp^2}$$

$$+ \frac{\alpha_s C_F}{2\pi^2} \frac{1}{K_\perp^2} \int_x^1 \mathrm{d}\xi \, \frac{1+\xi^2}{(1-\xi)_+} \frac{x}{\xi} q_{\mathbb{P}}\left(\frac{x}{\xi}, x_{\mathbb{P}}, K_\perp^2\right) \Bigg\} \exp\left[-S(K_\perp^2, Q^2)\right]$$

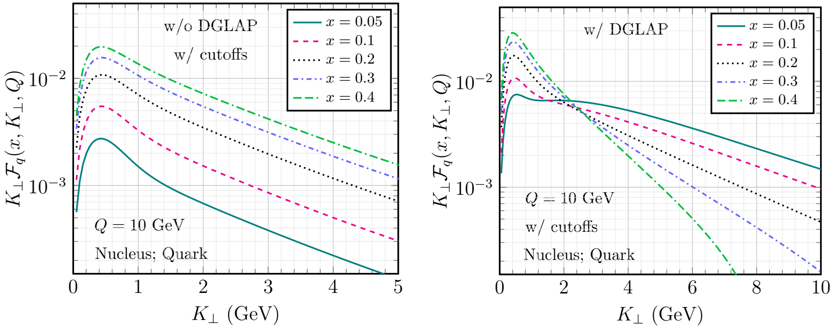

- The solution becomes negative for both quarks and gluons

Adding DGLAP: the negativity problem (2512.11730)

- The DGLAP solution enters the boundary condition for CSS

$$\mathcal{Q}_{\mathbb{P}}(x, x_{\mathbb{P}}, K_\perp^2, Q^2) = \Bigg\{ \mathcal{Q}_{\mathbb{P}}^{(0)}(x, x_{\mathbb{P}}, K_\perp^2) + \frac{\alpha_s C_F}{2\pi^2} \ln \frac{Q^2}{K_\perp^2} \frac{x q_{\mathbb{P}}\left(x, x_{\mathbb{P}}, P_\perp^2\right)}{K_\perp^2}$$

$$+ \frac{\alpha_s C_F}{2\pi^2} \frac{1}{K_\perp^2} \int_x^1 \mathrm{d}\xi \, \frac{1+\xi^2}{(1-\xi)_+} \frac{x}{\xi} q_{\mathbb{P}}\left(\frac{x}{\xi}, x_{\mathbb{P}}, K_\perp^2\right) \Bigg\} \exp\left[-S(K_\perp^2, Q^2)\right]$$

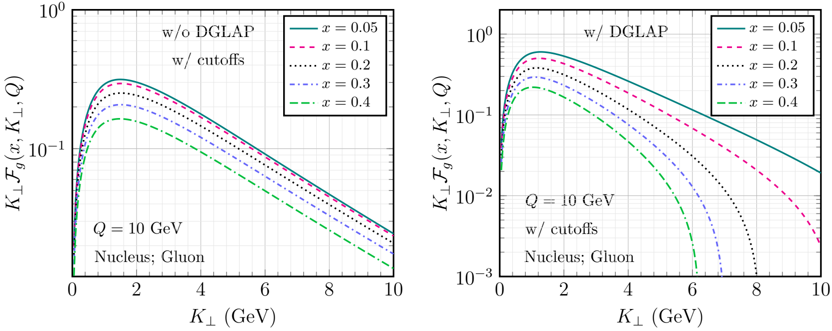

- A natural property of DGLAP evolution: $\partial \, x q_{\mathbb{P}}(x, K_\perp^2)/\partial \ln K_\perp^2 < 0$

Adding DGLAP: the negativity problem *(2512.11730)*

$$\mathcal{Q}_{\mathbb{P}}(x, x_{\mathbb{P}}, K_\perp^2, Q^2) = \Bigg\{ \mathcal{Q}_{\mathbb{P}}^{(0)}(x, x_{\mathbb{P}}, K_\perp^2) + \frac{\alpha_s C_F}{2\pi^2} \ln \frac{Q^2}{K_\perp^2} \frac{x q_{\mathbb{P}}\left(x, x_{\mathbb{P}}, P_\perp^2\right)}{K_\perp^2}$$

$$+ \frac{\alpha_s C_F}{2\pi^2} \frac{1}{K_\perp^2} \int_x^1 \mathrm{d}\xi \, \frac{1+\xi^2}{(1-\xi)_+} \frac{x}{\xi} q_{\mathbb{P}}\left(\frac{x}{\xi}, x_{\mathbb{P}}, K_\perp^2\right) \Bigg\} \exp\left[-S(K_\perp^2, Q^2)\right]$$

- CSS and DGLAP evolutions are consistent with each other via

$$x q_{\mathbb{P}}(x, x_{\mathbb{P}}, Q^2) \equiv \int^{Q^2} \mathrm{d}K_\perp^2 \, \mathcal{Q}_{\mathbb{P}}(x, x_{\mathbb{P}}, K_\perp^2, Q^2)$$

- Obtained via the small $\xi_0 \equiv K_\perp / Q$ expansion of a positive NLO correction

$$\mathcal{Q}_{\mathbb{P}}(x, x_{\mathbb{P}}, K_\perp^2, Q^2) = \Bigg\{ \mathcal{Q}_{\mathbb{P}}^{(0)}(x, x_{\mathbb{P}}, K_\perp^2) +$$

$$+ \frac{\alpha_s C_F}{2\pi^2} \frac{1}{K_\perp^2} \int_x^{1-\xi_0} \mathrm{d}\xi \, \frac{1+\xi^2}{1-\xi} \frac{x}{\xi} q_{\mathbb{P}}\left(\frac{x}{\xi}, x_{\mathbb{P}}, K_\perp^2\right) \Bigg\} \exp\left[-S(K_\perp^2, Q^2)\right]$$

- Why not use this positive expression?! Inconsistent with DGLAP!

- Consistency with DGLAP restored by appropriately changing the Sudakov

$$\mathcal{Q}_{\mathbb{P}}(x, x_{\mathbb{P}}, K_\perp^2, Q^2) = \Bigg\{ \mathcal{Q}_{\mathbb{P}}^{(0)}(x, x_{\mathbb{P}}, K_\perp^2) + + \frac{\alpha_s C_F}{2\pi^2} \frac{1}{K_\perp^2} \int_x^{1-\xi_0} \mathrm{d}\xi \, \frac{1+\xi^2}{1-\xi} \, \frac{x}{\xi} q_{\mathbb{P}} \left(\frac{x}{\xi}, x_{\mathbb{P}}, K_\perp^2 \right) \Bigg\} \exp\left[-S_{\rm pro}(K_\perp^2, Q^2)\right]$$

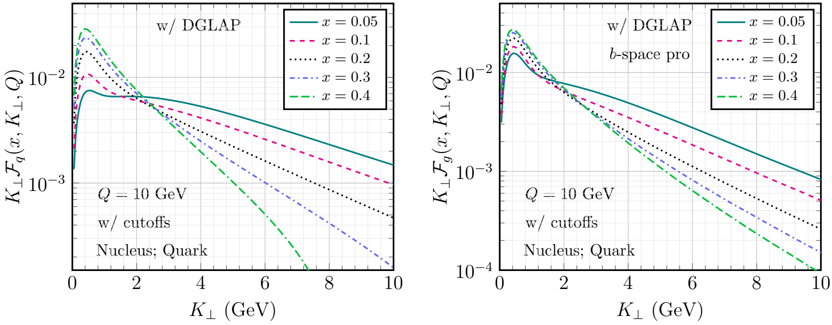

- The solution becomes positive for both quarks and gluons

- Consistency with DGLAP restored by appropriately changing the Sudakov

$$\mathcal{Q}_{\mathbb{P}}(x, x_{\mathbb{P}}, K_\perp^2, Q^2) = \Bigg\{ \mathcal{Q}_{\mathbb{P}}^{(0)}(x, x_{\mathbb{P}}, K_\perp^2) + \\ + \frac{\alpha_s C_F}{2\pi^2} \frac{1}{K_\perp^2} \int_x^{1-\xi_0} \mathrm{d}\xi \, \frac{1+\xi^2}{1-\xi} \frac{x}{\xi} q_{\mathbb{P}}\left(\frac{x}{\xi}, x_{\mathbb{P}}, K_\perp^2\right) \Bigg\} \exp\left[-S_{\rm pro}(K_\perp^2, Q^2)\right]$$

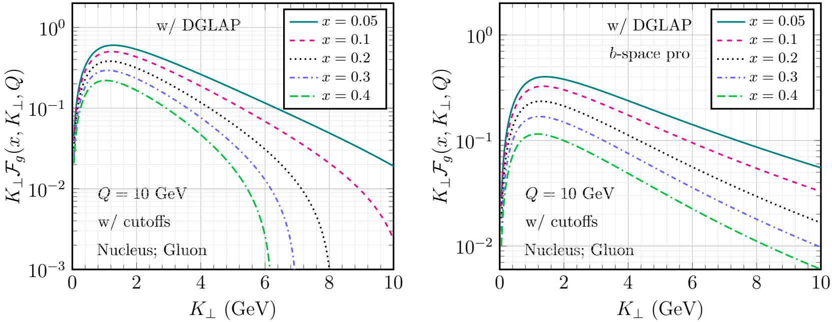

- DGLAP-guided resummation of power corrections $(K_\perp/Q)^n$ to all orders

- Compare CSS results with and without DGLAP: fixed x, various Q

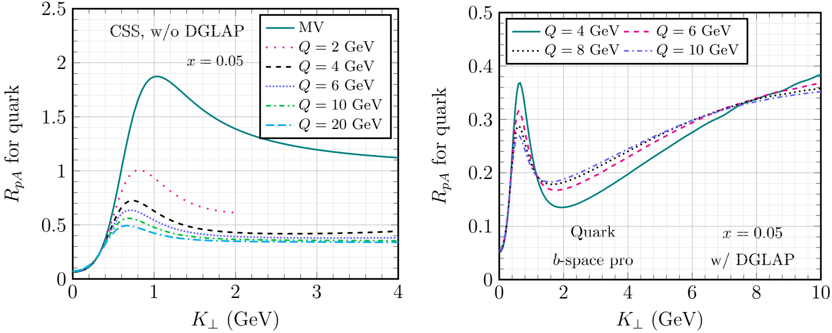

- The Cronin peak is somewhat smaller, but significantly more pronounced
- Large Q: the limiting value $1/A^{1/3}$ is gradually approached from below
- All hallmarks of saturation

- Compare CSS results with and without DGLAP: fixed x, various Q

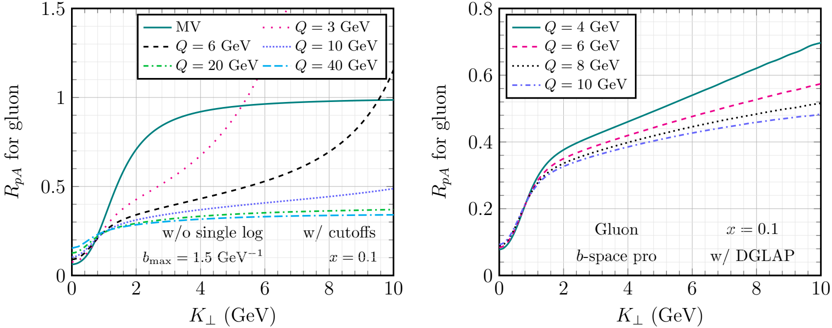

- With DGLAP, R_{pA} appears to be steadily increasing with $K_\perp$
- Proton evolves faster and thus gets depleted faster in a given bin of x
- With increasing Q, the difference between A and p evolutions diminishes
- Presumably the value $1/A^{1/3}$ is approached for large enough Q and $K_\perp$

The improved Sudakov *(Nefedov and Saleev, 2009.13188)*

- The PDF and the TMD are related via (say, for gluons)

$$xG(x,Q^2) \equiv \int^{Q^2} \mathrm{d}K_\perp^2\, \mathcal{F}(x,K_\perp^2,Q^2)$$

- The TMD takes the NLO structure (with $\xi_M \equiv \frac{Q}{Q+K_\perp}$)

$$\mathcal{F}(x,K_\perp^2,Q^2) = \left\{ \mathcal{F}^{(0)}(x,K_\perp^2) + \frac{\alpha_s}{2\pi^2}\frac{1}{K_\perp^2}\int_x^{\xi_M} \mathrm{d}\xi\, P_{gg}(\xi)\,\frac{x}{\xi}G\left(\frac{x}{\xi},K_\perp^2\right)\right\}\mathrm{e}^{-S}$$

- The PDF obeys the DGLAP equation with tree-level initial condition

- An equation for the improved Sudakov (analytically solved)

$$\frac{\mathrm{d}S}{\mathrm{d}\ln K_\perp^2} = \frac{\alpha_s(K_\perp^2)}{2\pi}\left\{\int_{\xi_M}^1 \mathrm{d}\xi\, P_{gg}(\xi)\left[\xi - \frac{(x/\xi)G(x/\xi,K_\perp^2)}{xG(x,K_\perp^2)}\right] - \int_0^{\xi_M} \mathrm{d}\xi\, \xi P_{gg}(\xi)\right\}$$

- When $K_\perp \ll Q$, the virtual piece yields the standard Sudakov

- Diffraction is arguably the high-energy process most sensitive to saturation
- CGC $\Rightarrow$ TMD factorisation for the diffractive production of hard jets
- At tree-level (MV model), the R_{pA} ratio exhibits strong saturation signals
    - suppression at $K_\perp < Q_s(A)$, Cronin peak in some cases

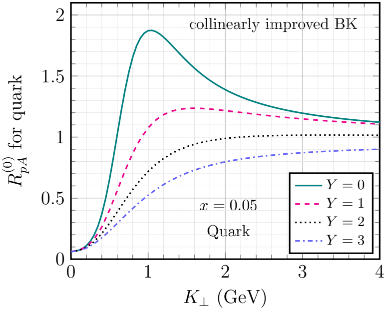

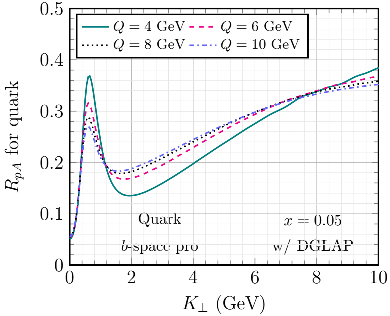

- Suppression at small $K_\perp$ is preserved by all evolutions
- Cronin peak is washed out by BK, but seems preserved by CSS/DGLAP